

## $\pi^+$ and $\pi^-$ momentum distribution normal to the production plane in the reaction $pp \rightarrow pp + \text{mesons}^*$

C. Ezell, A. T. Laasanen, and L. J. Gutay

*Physics Department, Purdue University, West Lafayette, Indiana 47907*

W. N. Schreiner and P. Schübelin,<sup>†</sup>

*Brookhaven National Laboratory, Upton, New York 11973*

F. Turkot

*Fermi National Accelerator Laboratory, Batavia, Illinois 60510*

(Received 9 October 1975)

The  $\pi^+$  and  $\pi^-$  momentum distribution normal to the production plane is studied. The dispersion of the momentum distribution normal to the production plane is independent of the transverse momenta of the trigger protons.

Seeking direct experimental evidence for the constituent structure of the proton is of current interest in high-energy physics. One possible approach to this problem is to study high-transverse-momentum ( $P_{\perp}$ ) reactions. This is based on the commonly accepted assumption that high  $P_{\perp}$  is a signature of close collision. This hypothesis needs further scrutiny since production of a large-mass fireball with isotropic decay distribution can also contribute to large- $P_{\perp}$  events. Although we cannot prove correct or rule out with certainty all constituent or fireball models, there are certain features of the data which can rule out that class of fireball or nova models for which the temperature increases with  $P_{\perp}$  or the multiplicity grows less than linearly with the fireball mass while the fireball mass grows at least linearly with  $P_{\perp}$ .

The experiment was carried out at the Brookhaven National Laboratory AGS with the Multiparticle ARGO Spectrometer System (MASS).<sup>1</sup> Using all three spectrometers, namely the high-momentum spectrometer (HMS), the low-momentum spectrometer (LMS), and the vertex spectrometer (VS),<sup>2</sup> we studied the reaction

$$p_1 + p_2 \rightarrow p_3 + p_4 + n\pi \quad (1)$$

at 28.5 GeV/c. The HMS was used to trigger upon, identify, and momentum-analyze a forward proton ( $p_3$ ). Proton ( $p_4$ ) was also identified and momentum-analyzed (by the LMS). The data reported here are 8726 events which cover  $1.3 < M < 6$  GeV and  $0 \leq P_{\perp} < 1.5$  GeV/c, where  $M$  denotes the missing mass to  $p_3$  ( $M_3$ ) or  $p_4$  ( $M_4$ ) and  $P_{\perp}$  is the transverse momentum of  $p_3$  ( $P_{\perp 3}$ ) or of  $p_4$  ( $P_{\perp 4}$ ). The VS, which consisted of nine cylindrical wire spark chambers surrounding the liquid hydrogen target in a 10-kG magnetic field, detected the remaining charged particles in all reactions. Spark asso-

ciation into tracks was performed by the track-recognition code PITRACK.<sup>3</sup> The events were fitted to a common vertex and were classified according to prong number (2–14 prongs).

Since in reaction (1) both protons are identified, one can define two production planes. For con-

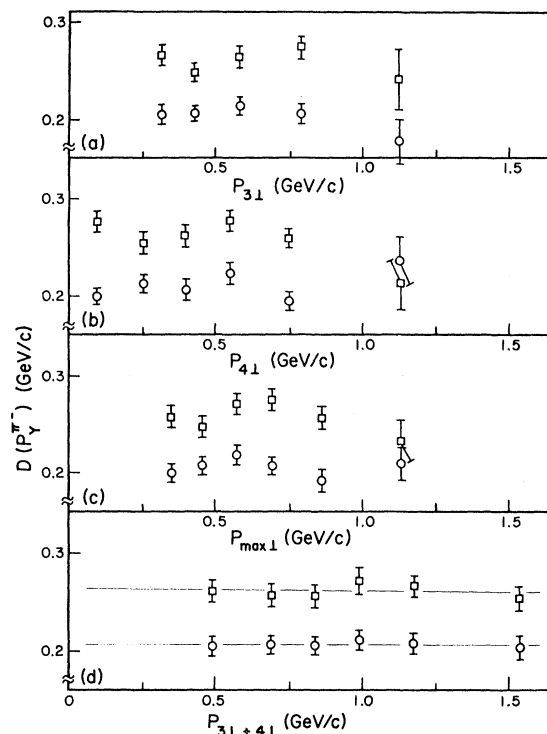


FIG. 1. Width of the negative-pion momentum distribution normal to the production plane for two  $X_{\pi^-}$  intervals as a function of (a)  $P_{\perp 3}$ , (b)  $P_{\perp 4}$ , (c)  $P_{\perp \max}$ , and (d)  $P_{\perp 3} + P_{\perp 4}$ . The symbols  $\circ$  and  $\square$  denote the intervals  $-0.025 < X_{\pi^-} \leq 0.025$  and  $0.025 < X_{\pi^-} \leq 0.100$ . In (d) the least-square fits of  $D(P_y^{\pi^-}) = a + b(P_{\perp 3} + P_{\perp 4})$  to the data are shown.

venience we choose  $\vec{p}_3 \times \vec{p}_1 / |\vec{p}_3 \times \vec{p}_1|$  as our production normal. (The small vertical aperture of the vertex magnet imposes approximate coplanarity of  $\vec{p}_3$  and  $\vec{p}_4$ .) In what follows we choose our  $Y$  and  $Z$  axes along the production normal and the incident beam direction, respectively. The choice of a right-handed coordinate system defines the  $X$  axis. The mean square deviation,  $D^2(P_y)$ , of  $P_y$  for the outgoing charged particle (other than  $p_3$  and  $p_4$ ) observed in VS is defined as

$$D^2(P_y^{\pi^\pm}) = \langle (P_y^{\pi^\pm} - \langle P_y^{\pi^\pm} \rangle)^2 \rangle.$$

We studied the functional dependence of  $D(P_y^{\pi^\pm}) = [D^2(P_y^{\pi^\pm})]^{1/2}$  on  $P_{\perp}$  in the  $-0.025 < X_{\parallel}^{\pi^\pm} \leq 0.025$ ,  $0.025 < X_{\parallel}^{\pi^\pm} \leq 0.100$ ,  $0.100 < X_{\parallel}^{\pi^\pm} \leq 0.200$ ,  $0.200 < X_{\parallel}^{\pi^\pm} \leq 0.400$ , and  $0.400 < X_{\parallel}^{\pi^\pm} \leq 1.0$  intervals, where  $X_{\parallel} = 2P_z^{c.m.}/\sqrt{s}$ . The symbols  $P_z^{c.m.}$  and  $s$  denote the  $Z$  component of the pion momentum and  $\sqrt{s}$  the total center-of-mass energy. The  $P_{\perp}$  dependence of  $D(P_y)$  for a fixed  $X$  value can be determined as a function of  $P_{13}$ ,  $P_{14}$ ,  $P_{1\max}$ , or  $P_{13} + P_{14}$  for both  $\pi^+$  and  $\pi^-$ , or for the combined distribution. In Figs. 1(a)–1(d) we present the  $P_y^{\pi^\pm}$  variation as a function of all four possible cases for the two smallest  $X_{\parallel}^{\pi^\pm}$  bins where we have the highest sta-

tistics. Inspection of the figure reveals no  $P_{\perp}$  dependence. The same is true for the other  $X_{\parallel}^{\pi^\pm}$  bins though the statistical errors are large. The data of Fig. 1(d) were fitted with straight lines giving slopes of  $0.000 \pm 0.010$  and  $-0.003 \pm 0.015$ , thus showing no  $P_{\perp}$  dependence of  $D(P_y^{\pi^\pm})$ . In Fig. 2  $D(P_y^{\pi^+})$  is plotted as a function of  $P_{14}$  for all  $X_{\parallel}^{\pi^+}$  intervals. The fitted lines are shown for the two smallest  $X_{\parallel}^{\pi^+}$  intervals; their slopes are  $0.021 \pm 0.017$  and  $0.012 \pm 0.017$ , which is again consistent with no  $P_{\perp}$  dependence. To improve our statistics in Fig. 3 we combined the  $\pi^+$  and  $\pi^-$  data and plotted  $D(P_y^{\pi^\pm})$  as a function of  $P_{31} + P_{41}$ . The fitted lines are shown for the lowest two  $X_{\parallel}^{\pi^\pm}$  intervals. Their slopes are  $0.012 \pm 0.007$  and  $0.013 \pm 0.010$ .

Although the data for the three higher  $X_{\parallel}^{\pi^\pm}$  lines fluctuate over a wide range of the dispersions  $D(P_y^{\pi^+})$  and  $D(P_y^{\pi^-})$  in Fig. 2 and Fig. 3, there is an indication of a slight  $P_{\perp}$  dependence at higher  $X_{\parallel}^{\pi^\pm}$ . To examine this further we show in Table I the results of the least-squares fits to the linear form,  $D(P_y) = a + bP_{\perp}$ , for each  $X_{\parallel}^{\pi^\pm}$  interval. We find an increase of the numerical values of the fitted slopes with increasing  $X_{\parallel}$ . However, their values are consistent with zero within errors thus indi-

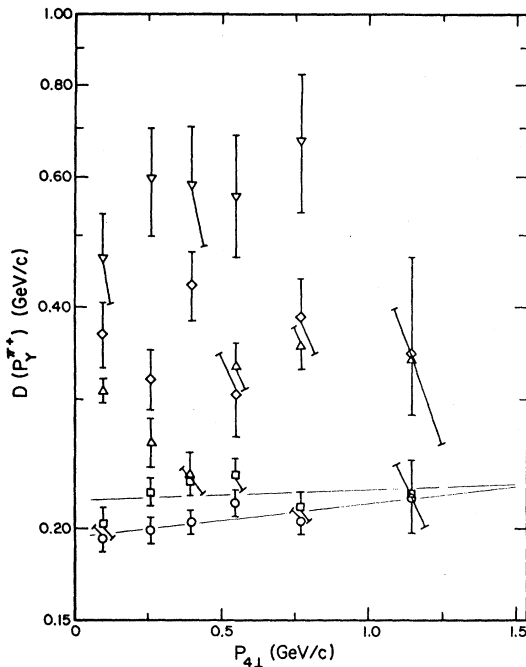


FIG. 2. Width of the positive-pion momentum distribution normal to the production plane for all  $X_{\parallel}^{\pi^+}$  intervals as a function of  $P_{14}$ . The symbols  $\circ$ ,  $\square$ ,  $\triangle$ ,  $\diamond$ , and  $\nabla$  denote the intervals  $-0.025 < X_{\parallel}^{\pi^+} \leq 0.025$ ,  $0.025 < X_{\parallel}^{\pi^+} \leq 0.100$ ,  $0.100 < X_{\parallel}^{\pi^+} \leq 0.200$ ,  $0.200 < X_{\parallel}^{\pi^+} \leq 0.400$ , and  $0.400 < X_{\parallel}^{\pi^+} \leq 1.0$ . The least-squares fit of  $D(P_y^{\pi^+}) = a + bP_{14}$  to the data are shown for the two lowest  $X_{\parallel}^{\pi^+}$  intervals.

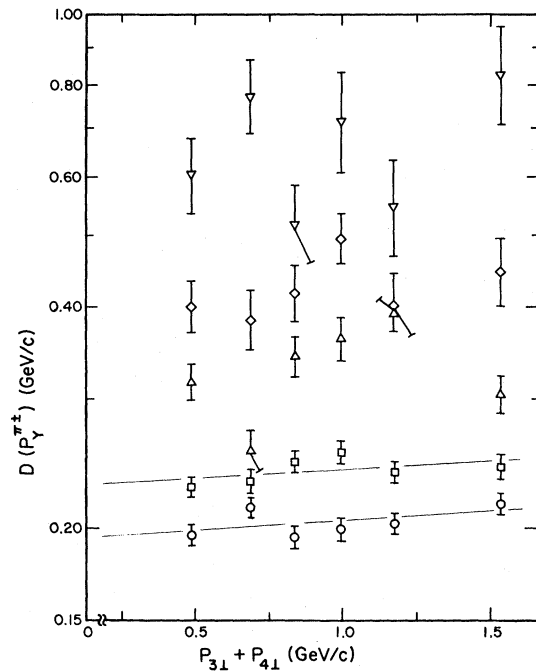


FIG. 3. Width of the positive- and negative-pion momentum distribution normal to the production plane for all  $X_{\parallel}^{\pi^\pm}$  intervals as a function of  $P_{31} + P_{41}$ . The symbols  $\circ$ ,  $\square$ ,  $\triangle$ ,  $\diamond$ , and  $\nabla$  denote the intervals  $-0.025 < X_{\parallel}^{\pi^\pm} \leq 0.025$ ,  $0.025 < X_{\parallel}^{\pi^\pm} \leq 0.100$ ,  $0.100 < X_{\parallel}^{\pi^\pm} \leq 0.200$ ,  $0.200 < X_{\parallel}^{\pi^\pm} \leq 0.400$ , and  $0.400 < X_{\parallel}^{\pi^\pm} \leq 1.0$ . The least-squares fits of  $D(P_y^{\pi^\pm}) = a + b(P_{31} + P_{41})$  to the data are shown for the two lowest  $X_{\parallel}^{\pi^\pm}$  intervals.

TABLE I. Results of least-square fits to the data of Figs. 1–3 of the form  $D(P_y) = a + bP_{\perp}$ . For the meaning of the symbols in the fourth column, see the figure captions.

Figure	$P_{\perp}$	$D(P_y)$	$X_{\parallel}^{\pi^{\pm}}$	$a$ (GeV/c)	$b$	$\chi^2/N$
1(a)	$P_{\perp 3}$	$D(P_y^{\pi^-})$	○	$0.218 \pm 0.007$	$-0.026 \pm 0.011$	4.17/3
			□	$0.245 \pm 0.015$	$0.019 \pm 0.027$	4.13/3
1(b)	$P_{\perp 4}$	$D(P_y^{\pi^-})$	○	$0.203 \pm 0.006$	$0.003 \pm 0.012$	7.67/4
			□	$0.270 \pm 0.010$	$-0.032 \pm 0.018$	3.26/4
1(c)	$P_{\perp \text{ max}}$	$D(P_y^{\pi^-})$	○	$0.207 \pm 0.010$	$-0.005 \pm 0.015$	4.59/4
			□	$0.260 \pm 0.015$	$-0.008 \pm 0.023$	5.73/4
1(d)	$P_{\perp 3} + P_{\perp 4}$	$D(P_y^{\pi^-})$	○	$0.205 \pm 0.010$	$0.000 \pm 0.010$	0.20/4
			□	$0.259 \pm 0.015$	$-0.003 \pm 0.015$	1.42/4
2	$P_{\perp 4}$	$D(P_y^{\pi^+})$	○	$0.194 \pm 0.006$	$0.021 \pm 0.012$	2.67/4
			□	$0.216 \pm 0.009$	$0.012 \pm 0.017$	6.28/4
			△	$0.254 \pm 0.018$	$0.086 \pm 0.038$	18.0/4
			◇	$0.345 \pm 0.031$	$0.005 \pm 0.069$	6.68/4
			▽	$0.463 \pm 0.077$	$0.269 \pm 0.200$	0.72/3
3	$P_{\perp 3} + P_{\perp 4}$	$D(P_y^{\pi^+})$	○	$0.192 \pm 0.007$	$0.012 \pm 0.007$	8.63/4
			□	$0.226 \pm 0.010$	$0.013 \pm 0.010$	4.61/4
			△	$0.288 \pm 0.021$	$0.033 \pm 0.021$	31.6/3
			◇	$0.374 \pm 0.045$	$0.052 \pm 0.048$	3.97/4
			▽	$0.577 \pm 0.106$	$0.051 \pm 0.117$	8.59/4

cating no significant dependence of the momenta distribution on  $P_{\perp}$  of the trigger protons.

This observation of nearly constant width of the distribution of pion momenta normal to the production plane with increasing  $P_{\perp}$  of a trigger proton contradicts two classes of single-fireball models: those for which the temperature increases with the  $P_{\perp}$  of the trigger protons and those for which the multiplicity grows less than linearly with the fireball mass<sup>4</sup> while the fireball mass increases at least linearly with  $P_{\perp}$ . Each of these classes of models requires an increase of the mo-

menta of the secondary particles normal to the production plane. However, our results are in agreement with either the hard-scattering models or small-fireball models<sup>5</sup> and support earlier results obtained from the momentum distribution of the negative pions in the reaction  $pp \rightarrow p + X$ .<sup>6</sup>

We would like to thank our collaborators at Brookhaven National Laboratory, Virginia Polytechnic Institute and State University and the University of Wisconsin for their efforts in data-taking and reduction.

\*Work supported in part by the U. S. Energy Research and Development Administration.

†Present address: Centre de Recherches Nucléaires, Strasbourg, France.

<sup>1</sup>J. R. Ficenece *et al.*, *Experimental Meson Spectroscopy*, edited by C. Baltay and A. Rosenfeld (Columbia Univ. Press, New York, 1970), p. 581.

<sup>2</sup>J. R. Ficenece *et al.*, Nucl. Instrum. Meth. **113**, 535 (1973).

<sup>3</sup>D. R. Gilbert *et al.*, Nucl. Instrum. Meth. **116**, 501

(1974).

<sup>4</sup>J. D. Bjorken, in Proceedings of the Second International Conference on Elementary Particles, Aix-en-Provence, 1973 [J. Phys. (Paris) Suppl. **34**, C1-385 (1973)].

<sup>5</sup>S. D. Ellis and R. Thun, in *Proceedings of the IXth Rencontre de Moriond*, edited by J. Tran Thanh Van (Université de Paris-Sud, Orsay, 1974), Vol. I, p. 37.

<sup>6</sup>T. S. Clifford *et al.*, Phys. Rev. Lett. **34**, 978 (1975).